Tumor Necrosis Factor-α-mediated Regulation of the Inositol 1,4,5-Trisphosphate Receptor Promoter*

Keigan M. Park[‡§]**, David I. Yule**[§]**, and William J. Bowers**[‡¶1]

From the ¶*Department of Neurology,* ‡*Center for Neural Development and Disease, and* §*Department of Pharmacology and Physiology, School of Medicine and Dentistry, University of Rochester Medical Center, Rochester, New York 14642*

Tumor necrosis factor-α (TNF-α), a proinflammatory cytokine, has been implicated as a central mediator in multiple homeostatic and pathologic processes. Signaling cascades downstream of its cellular cognate receptors, as well as the resultant transcriptional responses have received intense interest in regards to how such signals impact cellular physiology. Notably, TNF-α was shown to potentiate neuronal Ca^{2+} signaling by enhancing type-1 inositol 1,4,5-trisphosphate receptor (IP_3R) steady-state mRNA levels. In the present study, we sought to determine the promoter region ultimately responsive to TNF-α exposure. We report that a sequence encompassing a specificity protein 1 (SP-1) binding site is necessary for TNF-α regulation. Electrophoretic mobility shift analysis demonstrated specific binding to this sequence, while site-directed mutagenesis of this site abrogated both JNK-mediated regulation as well as transcription factor binding. Expression of a dominant-negative SP-1 eliminated both the enhanced promoter activity and the elevated IP_3R-mediated Ca^{2+} signals observed with TNF-α exposure. Overall, these data delineate a key pathway by which TNF-α in a neuronal environment modulates IP_3R expression and intracellular Ca^{2+} homeostasis.

Neuroinflammation has been intimately linked to several prominent neurological diseases including Alzheimer, Parkinson, and Multiple Sclerosis (reviewed in Ref. 1). Central to the observed pathological neurodegeneration in these prior studies, is the abnormal production of pro-inflammatory cytokines, including tumor necrosis factor-α (TNF-α)[2] and interleukin-1 (IL-1) (reviewed in Ref. 2).

TNF-α was first described as a protein component of serum that exhibited potent antitumor activity (3). The 212-amino acid transmembrane pro-form, which is active during direct cell to cell contact, is expressed on the plasma membrane (4). This precursor protein is subsequently cleaved into a soluble TNF-α molecule by TNF-α-cleaving enzyme (TACE). TNF-α then signals in both an autocrine and paracrine fashion (5). It is this latter form that has been studied as an important immuno-modulating agent both in inflammatory processes in the peripheral immune system and in the central nervous system even in the absence of immune cell infiltration (6).

The two major receptors for TNF-α, p55 (TNF-RI) and p75 (TNF-RII) are expressed on the surface of neurons both *in vitro* and *in vivo* (7). Binding of homotrimeric TNF-α to either receptor can activate three important signaling pathways: the TNF receptor-associated death domain (TRADD), and the nuclear factor κB (NFκB) and Jun N-terminal kinase (JNK) signaling cascades. Through this diverse signaling array, TNF-α can regulate many physiologically important pathways in neurons. These include the regulation of cell survival, the initiation of apoptosis, synaptic transmission, and the alteration of gene expression (8–11).

Cells can also regulate diverse biological processes through the regulation of intracellular ions. Specifically, increases in cytosolic Ca^{2+} can regulate gene transcription, membrane excitability, muscle contraction, and neurotransmitter release (12). Conceptually, the amplitude and frequency of these Ca^{2+} signals can be altered in three basic ways: through the modulation of the amount of Ca^{2+} allowed to pass through an individual channel, by the intracellular location of the channel and through the number of channels present. Our laboratory, as well as others, have previously elucidated the means by which the extent of Ca^{2+} released from the inositol 1,4,5-trisphosphate receptor (IP_3R), a major intracellular Ca^{2+} release channel, can be regulated by ATP binding and phosphorylation (13–16). In addition, we have also explored mechanisms by which IP_3R density and cellular localization can dramatically affect intracellular Ca^{2+} waves (17). In contrast, the possible role that transcriptional control of IP_3R expression may impart on endoplasmic reticulum (ER)-derived Ca^{2+} signals has been relatively understudied.

Recently, we reported evidence for cross-talk between the TNF-α and IP_3R signaling pathways that indicated a role for receptor expression in defining the extent of Ca^{2+} release. It was shown that TNF-α regulates IP_3R-mediated Ca^{2+} signals in primary murine cortical neurons via a JNK-dependent increase in IP_3R protein levels (18). This marked enhancement of Ca^{2+} signals has implications for neuronal excitability since altered ER Ca^{2+} release can profoundly influence plasma membrane potential (19) and can eventually undermine long-term neuronal viability (20).

In the present study, we examined the JNK-dependent regulation of type-1 IP_3R mRNA expression by TNF-α at the level of

[1] To whom correspondence should be addressed: 601 Elmwood Ave., Box 645, Rochester, NY 14642. Tel.: 585-273-2195; Fax: 585-276-1947; E-mail: william_bowers@urmc.rochester.edu.

[2] The abbreviations used are: TNF, tumor necrosis factor; JNK, c-Jun N-terminal kinase; IL, interleukin; ER, endoplasmic reticulum; IP_3R, inositol 1,4,5-trisphosphate receptor; EMSA, electrophoretic mobility shift assay; ANOVA, analysis of variance; GST, glutathione S-transferase; DN, dominant-negative; CICR, calcium-induced calcium release.

the type-1 IP$_3$R promoter. We report that a functional specificity protein 1 (SP-1) transcription factor binding site exists within the human type-1 IP$_3$R promoter and that mutation of this binding site eliminates both JNK regulation and the binding of SP-1. Regulation of IP$_3$R expression during periods of TNF-α induced neuroinflammatory responses, especially those that arise in the context of progressive neurodegenerative diseases, may contribute to a cellular environment prone to dysfunction and/or death.

EXPERIMENTAL PROCEDURES

Cell Culture—Neuro2A (ATCC Manassas, VA) cells, passages 2–20, were cultured in Dulbecco's modified Eagle's medium (Invitrogen) plus 8% fetal bovine serum (Gemini, West Sacramento, CA) in a T75 flask (Corning, Corning, NY). Cell transfection was performed using a nucleofection system (Amaxa, Gaithersburg, MD) according to the manufacturer's instructions. Briefly, cells were trypsinized, resuspended in growth medium, and enumerated. One million cells were then added to a tube containing a total of 5 μg of plasmid DNA. The Neuro2A cells were then subjected to nucleofection and plated in 12-well culture dishes (Corning). Addition of murine recombinant tumor necrosis factor-α (TNF-α; Peprotech, Rocky Hill, NJ) was performed prior to analysis as indicated. Transfected cells designated for luciferase assays were subsequently lysed with Passive Lysis Buffer (Promega, Madison, WI), and samples were stored at $-80\,°C$.

Calcium Imaging—Neuro2A cells were plated on glass coverslips (Carolina, Burlington, NC) for 48 h in 12-well culture dishes (Corning). Twenty-four hours before imaging, 100 ng/ml of murine recombinant TNF-α or phosphate-buffered saline, as a negative control, was added to the culture medium. A subset of cultures was pretreated for 1 h with 10 μM SP600125 before cytokine addition. Neuro2A cells were loaded with 1 μM of the Ca^{2+}-sensitive dye Fura2-AM (TEFLABS, Austin, TX) for 15 min at 37 °C. During this time, ryanodine (100 μM) was loaded for the RyR blocking experiment. The cells were then perfused with a physiological salt solution containing in mM: 5.5 glucose, 0.56 MgCl$_2$, 2 KCl, 1 Na$_2$HP0$_4$, 10 HEPES, and 1.2 CaCl$_2$, pH 7.4 or a La^{3+}-Ca^{2+} reduced solution (300 μM La^{3+} with 0.5 mM Ca^{2+}) during store size analysis. Addition of bradykinin (Sigma) to elicit a Ca^{2+} response was accomplished using a gravity-fed system (Warner Instruments, Camden, CT) while 340/380 nm excitation was provided by a Polychrome V monochrometer illumination system under the control of TILL Vision software. Emitted fluorescence was captured using a SENSICAM-QE (Cooke, Romulus, MI) camera at a sampling rate of 1 Hz. Peak height of the 340/380 ratio from baseline in the presence of the agonist for each Neuro2A cell in the field was averaged for each coverslip (n). A signal more than two standard deviations from the baseline 340/380 ratio was considered a response.

Quantitative Real-time RT-PCR—Total RNA was purified from Neuro2A cells using the TRIzol (Invitrogen) phenol-chloroform method. A High-Capacity cDNA archiving kit (Applied Biosystems, Foster City, CA) was utilized to convert 2 μg of RNA into cDNA. Quantification of type-1 IP$_3$R mRNA levels was then obtained by comparison of sample reactivity to that of a serially diluted type-1 IP$_3$R plasmid in the presence of an Assay-on-Demand primer/probe set (Mm00439917, Applied Biosystems). An 18S rRNA-specific primer/probe set was used as an internal control. To inhibit JNK activity, 10 μM SP600125 was added 1 h before the addition of 100 ng/ml of recombinant TNF-α.

Western Blotting—Neuro2A cells were lysed in a modified radioimmune precipitation assay buffer (50 mM Tris-HCL, 1% Nonidet P-40, 150 mM NaCl, 0.25% sodium deoxycholate, 1 mM EDTA, pH 7.4) containing 1$\times$ protease inhibitor mixture (Sigma) and homogenized through a 21.5-gauge needle. Protein quantification was accomplished by an Amido Black assay (21). The lysates were then subjected to SDS-PAGE and transferred to a polyvinylidene difluoride membrane. The membrane was then incubated with type-1 IP$_3$R (1:1000, Chemicon), and β-actin (1:2000, Sigma) antibodies for 2 h, which were subsequently detected with affinity-purified, horseradish peroxidase-conjugated donkey anti-rabbit/mouse antibodies (1:5000, Sigma) in combination with Western Lightning reagent (PerkinElmer Life Sciences). Band intensities were quantified using Labworks software and presented as OD ratios of IP$_3$R to β-actin.

IP$_3$R Promoter-driven Reporter Plasmids and JNK- and NFκB-activating Constructs—Type-1 human IP$_3$R promoter constructs were kindly provided by Dr. Peter Sims (University of Rochester, Rochester, NY) (22). These constructs each contained a defined segment of the IP$_3$R promoter inserted into the pGL3 vector (Promega) upstream of the firefly luciferase reporter gene. Numbers designated in the name assigned to each reporter plasmid indicate the distance from the transcriptional start site of the IP$_3$R gene. The ΔMEKK and p65 expression plasmids were kindly provided by Dr. Dirk Bohmann (University of Rochester) and Dr. Sanjay Maggirwar (University of Rochester), respectively (23, 24). The dominant-negative SP-1 construct and respective control was provided by Gerald Thiel (Saarland Medical Center, Homburg, Germany) (25).

Luciferase Activity Measurements—Neuro2A cell lysates were analyzed using the Dual-Luciferase® Reporter assay (Promega) in accordance with the manufacturer's directions. Briefly, 20 μl of cell lysate was added to a 96-well Black Bottom Plate (Corning), and room temperature luciferase reagent was added to each well. A Lumicount luminescent plate reader (Packard, Downers Grove, IL) was first used to monitor firefly luciferase activity and then *Renilla* luciferase activity after the addition of a Stop and Glo® reagent (Promega). *Renilla* expression was used as an internal transfection control, levels of which remained unchanged in each of the transfection experiments.

Site-directed Mutagenesis—Sites within the type-1 IP$_3$R promoter that were predicted to be regulated by JNK were mutated using the QuikChange site-directed mutagenesis kit (Stratagene). The sequences that were altered are as follows; -252 was altered from 5′-GACTTTGAAC-3′ to 5′-CCTCCCCCCT-3′ and $+59$ and $+125$ were altered from 5′-GAGAGGA-3′ to 5′-TGTGTTG-3′.

Electrophoretic Mobility Shift Assay—Nuclear lysates were obtained by mechanically disrupting Neuro2A cells in a sucrose solution containing 0.5% Nonidet P-40. A salt gradient (increasing KCl) method was used to separate the cytosolic proteins from nuclear extracts. Resultant nuclear preparations

were tested for their ability to bind to a 42-bp oligonucleotide probe formed by the annealing of two synthesized primers encompassing the +38 to +80 region of the type-1 IP$_3$R promoter and labeled with α-^{32}P-labeled deoxynucleotides. The primer sequences were the following: Sense strand 5′-GGGGT-GGGAG**GAGAGGA**GGAGGAGGAG-3′; antisense strand 5′-CCACCTCCTCCTCC**TCCTCTC**CTCCCA-3′. A ^{32}P-labeled mutant probe was also generated that contained the sequence 5′-TGTGTTG-3′ to replace the wild-type sequence 5′-GAGAGGA-3′. The nuclear extracts were incubated for 30 min at 22 °C with the probe in the presence of poly(dIdC) and binding buffer (50 mM Tris HCl, 750 mM KCl, 2.5 mM EDTA, 1 mM dithiothreitol, 0.5% Triton X-100, and 62.5% glycerol). In antibody competition assays, SP-1 and c-Fos antibodies (Millipore, Billerica, MA) were added at the time of probe incubation. The samples were then subjected to electrophoresis on a 5% non-denaturing polyacrylamide gel. Exposures were obtained by subjecting the dried gel to autoradiography film (GE Healthcare, Piscataway, NJ).

RESULTS

TNF-α Enhances IP$_3$R-mediated Ca^{2+} Signals and mRNA Levels in Neuro2A Cells—Previously, we reported that the proinflammatory cytokine TNF-α enhanced Ca^{2+} signals in primary cortical neurons (18). In an effort to find a suitable cell model for determining the mechanism responsible for the enhanced mRNA levels, we examined the effects of TNF-α in the Neuro2A murine neuroblastoma cell line. Neuro2A cells were plated on glass coverslips and subsequently subjected to Ca^{2+} imaging. A 24-h pretreatment with 100 ng/ml TNF-α led to a significant up-regulation of bradykinin-induced cytosolic Ca^{2+} signals (Fig. 1, *A* and *B*). In agreement with our previous studies, these augmented signals were also sensitive to the JNK inhibitor SP600125 (Fig. 1, *A* and *B*). The ability of JNK activity to directly regulate IP$_3$R-mediated Ca^{2+} signals was also assayed by the transient transfection of ΔMEKK1, a truncated MEKK construct that leads to the phosphorylation and subsequent activation of JNK (26). ΔMEKK1 was nucleofected into Neuro2A cells 24 h before Ca^{2+} imaging (Fig. 1, *C* and *D*), and the transfection efficiency was monitored by the co-transfection of hcRed. Fluorescence monitoring indicated ~50% of the cells in the field of view were transfected (data not shown). Again, Ca^{2+} signals downstream of bradykinin activation were enhanced in the presence of ΔMEKK1, suggesting JNK can regulate IP$_3$R-mediated Ca^{2+} signaling in this neuronal cell line.

It was previously reported that the TNF-α-mediated enhancement of IP$_3$R-derived Ca^{2+} signals in primary neurons was independent of alterations in calcium-induced calcium release (CICR) or differences in ER store loading (18). CICR occurs when Ca^{2+} released from the IP$_3$R increases the open probability of proximal ryanodine receptors (RyR). To disable this coupling and examine the possible role of CICR in the cytokine enhanced bradykinin-induced Ca^{2+} signals, ryanodine was added to the Neuro2A cells prior to Ca^{2+} imaging. The addition of the CICR blocker did not alter the enhanced bradykinin signals, suggesting CICR was not responsible for the effect (Fig. 1, *E* and *F*). Augmented ER Ca^{2+} loading could also enhance IP$_3$R-mediated Ca^{2+} release. To measure the amount

of Ca^{2+} in the ER store, cyclopiazonic acid (CPA), which induces passive leak from ER stores by blocking SERCA pump activity, was added in the presence of a Ca^{2+} entry blocking solution containing La^{3+}. In agreement with our previous findings, there was no alteration in the levels of Ca^{2+} within the ER following TNF-α addition (Fig. 1, *G* and *H*).

Our previous data had also indicated that in primary neurons, an increase in type-1 IP$_3$R mRNA positively correlated with this induction. To measure type-1 IP$_3$R mRNA, Neuro2A cells were treated with recombinant TNF-α or phosphate-buffered saline and mRNA was purified at various time points. Real-time quantitative RT-PCR revealed a significant increase (3-fold, $p = 0.01$) in type-1 IP$_3$R mRNA levels 8 h after cytokine addition (Fig. 1*I*). This enhancement in IP$_3$R mRNA was also sensitive to SP600125 (Fig. 1*J*) and correlated with an increase in type-1 protein 24 h after cytokine addition (Fig. 1, *K* and *L*).

In aggregate, the observed increase in Ca^{2+} signals as a result of direct JNK activation, the enhanced type-1 IP$_3$R mRNA, protein, and Ca^{2+} signals with TNF-α incubation suggests that Neuro2A cells express a homologous signaling pathway to that observed in primary neurons and represent an appropriate cell model for examining the effects of TNF-α on IP$_3$R promoter activity.

TNF-α Regulates the Activity of the Type-1 IP$_3$R Promoter—A reporter plasmid consisting of a 772-bp segment of the human type-1 IP$_3$R promoter lying upstream of the luciferase gene was transiently transfected into Neuro2A cells to assay for an increase in promoter activity following TNF-α exposure. A significant increase in luciferase activity was observed 3 h after cytokine addition, which was maintained at the 6-h time point, and returned to baseline by 12 h (Fig. 2*A*). This suggested a temporal regulation of IP$_3$R promoter activity via TNF-α-dependent signaling. We next sought to determine the region of the IP$_3$R promoter that was responsive to TNF-α activation. Three overlapping promoter constructs spanning −582, −252, and −9 bp from the transcriptional start site to +190 bp after the initiation site of the human IP$_3$R gene locus were transfected into Neuro2A cells. TNF-α incubation led to activation of luciferase expression from all three constructs to a similar degree, indicating the site of regulation lies within the shortest common promoter region, −9 to +190 (Fig. 2*B*).

The −9 to +190 Promoter Region Is Sufficient for JNK Activation of Transcription—TNF-α, through activation of its cell surface receptors TNF-RI and TNF-RII, has been linked to two major transcriptional regulatory cascades, JNK and NFκB. In an effort to more precisely implicate the pathway involved, we activated JNK and NFκB directly using a molecularly based approach. To confirm the ability of the ΔMEKK1 and p65 plasmids to activate JNK and NFκB in Neuro2A cells, we transiently co-transfected the plasmids with luciferase reporter constructs harboring concatenated consensus binding sites for AP-1 and NFκB (Fig. 3, *A* and *B*). After the specificity and ability of these constructs to activate their respective pathways was verified, the truncated type-1 IP$_3$R promoter-driven luciferase plasmids were co-transfected. Only ΔMEKK1 co-transfection significantly enhanced luciferase expression from all three reporter constructs (Fig. 3*C*) indicating that the regulatory site(s)
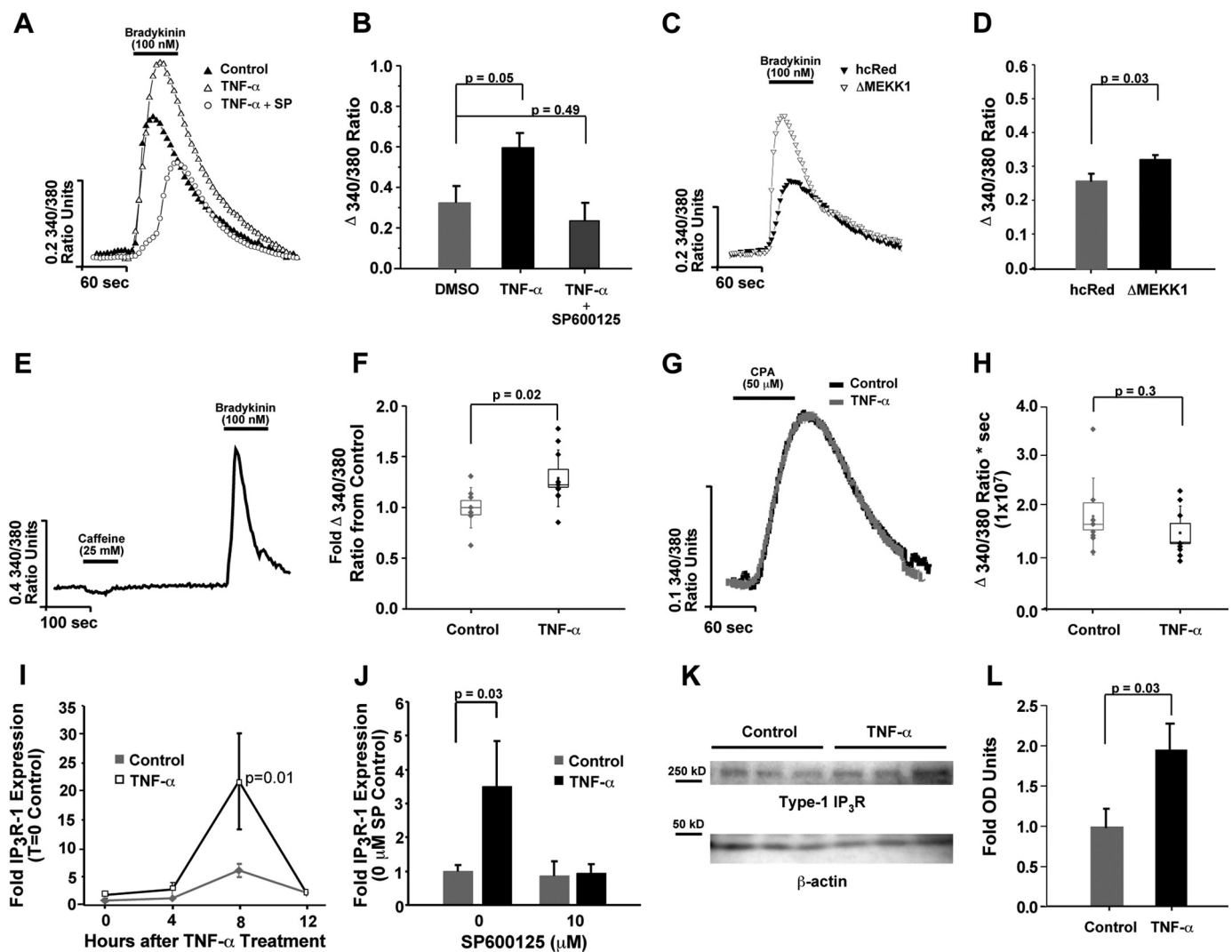
FIGURE 1. **TNF-α enhances Ca²⁺ mobilization in Neuro2A cells.** Neuro2A cells were treated with TNF-α for 24 h in the presence and absence of the JNK inhibitor (SP600125), and Ca²⁺ imaging was performed. *A*, traces of the emitted fluorescence after 340/380 nm excitation with bradykinin stimulation, an IP₃-generating agonist, were formed by averaging the responses from each Neuro2A cell in the field of view. SP600125 (10 μM) was added to the culture medium 1 h before TNF-α addition. *B*, coverslip averages for each treatment group ($n = 8$) are presented in bar graph form. *C*, *traces* are shown depicting enhanced responses in the presence of the JNK activator, ΔMEKK. *D*, overall averages are presented in bar graph form. *E* and *F*, Neuro2A cells were loaded with ryanodine (100 μM) to block the RyR and subjected to Ca²⁺ imaging. *E*, *trace* is shown illustrating the absence of a caffeine-induced Ca²⁺ signal, indicating successful block of the RyR. Box plot parameters: *dots* represent coverslip averages, the *center* of the box is the mean of the data, the *edge* of the box is one S.E., *whiskers* are one S.D. *F*, similar cytokine-induced enhancement in bradykinin signals suggested RyR coupling is not responsible for the effect. *G* and *H*, Ca²⁺ stores were measured using the cyclopiazonic acid leak method (in 300 μM La³⁺-reduced Ca²⁺ external solution), and total Ca²⁺ released by the area under the curve method is shown. *I*, total RNA from TNF-α-treated and untreated cultures was isolated at 0, 4, 8, and 12 h after cytokine addition. cDNA was subsequently prepared and quantitative real-time RT-PCR performed to determine the steady-state levels of the type-1 IP₃R mRNA with TNF-α treatment. Transcript expression changes are depicted as fold-change as compared with values obtained from the 0-h control time point. *J*, total RNA from TNF-α-treated and control cultures was isolated at 8 h after cytokine addition, but in the absence or in the presence of SP600125. Transcript expression changes are depicted as fold-change as compared with values obtained from the untreated control condition. *K* and *L*, type-1 IP₃R protein levels were analyzed via Western blotting and OD measurements are shown. *Error bars* represent 1 S.E., and *p* values were obtained using two-tailed Student's *t*-test.

responsive to both TNF-α and JNK activation lies within the −9 to +190 bp region.

+59-bp Site within IP₃R Promoter Is Responsible for JNK Regulation—*In silico* examination of the IP₃R promoter DNA sequence with transcription factor binding site prediction software AliBaba (version 2.1) and Genomatix's MatInspector, along with information garnered from Deelman *et al.* (27) suggested three putative JNK-regulated sites. A predicted AP-1 site was located outside the region of interest at −252 bp, and two possible AP-1 or SP-1 sites were mapped to the −9 to +190 bp region at +59 and +125 relative to the IP₃R transcriptional

start site (Fig. 4*A*). Site-directed mutagenesis of the core sequence at each of these sites was performed, and the effect of these mutations on promoter activity in the presence of the JNK activator ΔMEKK1 was determined. Mutation of the −252 bp site did not affect ΔMEKK1-mediated enhancement of luciferase activity as expected from the previous experiments using the truncated promoter plasmids (Fig. 4*B*). Similarly, ablation of the +125bp site did not alter ΔMEKK1-mediated enhancement (Fig. 4*C*). In contrast, mutation of the +59 site abolished the enhancement in luciferase activity following ΔMEKK1 expression (Fig. 4*D*). This finding suggested that the site(s) of
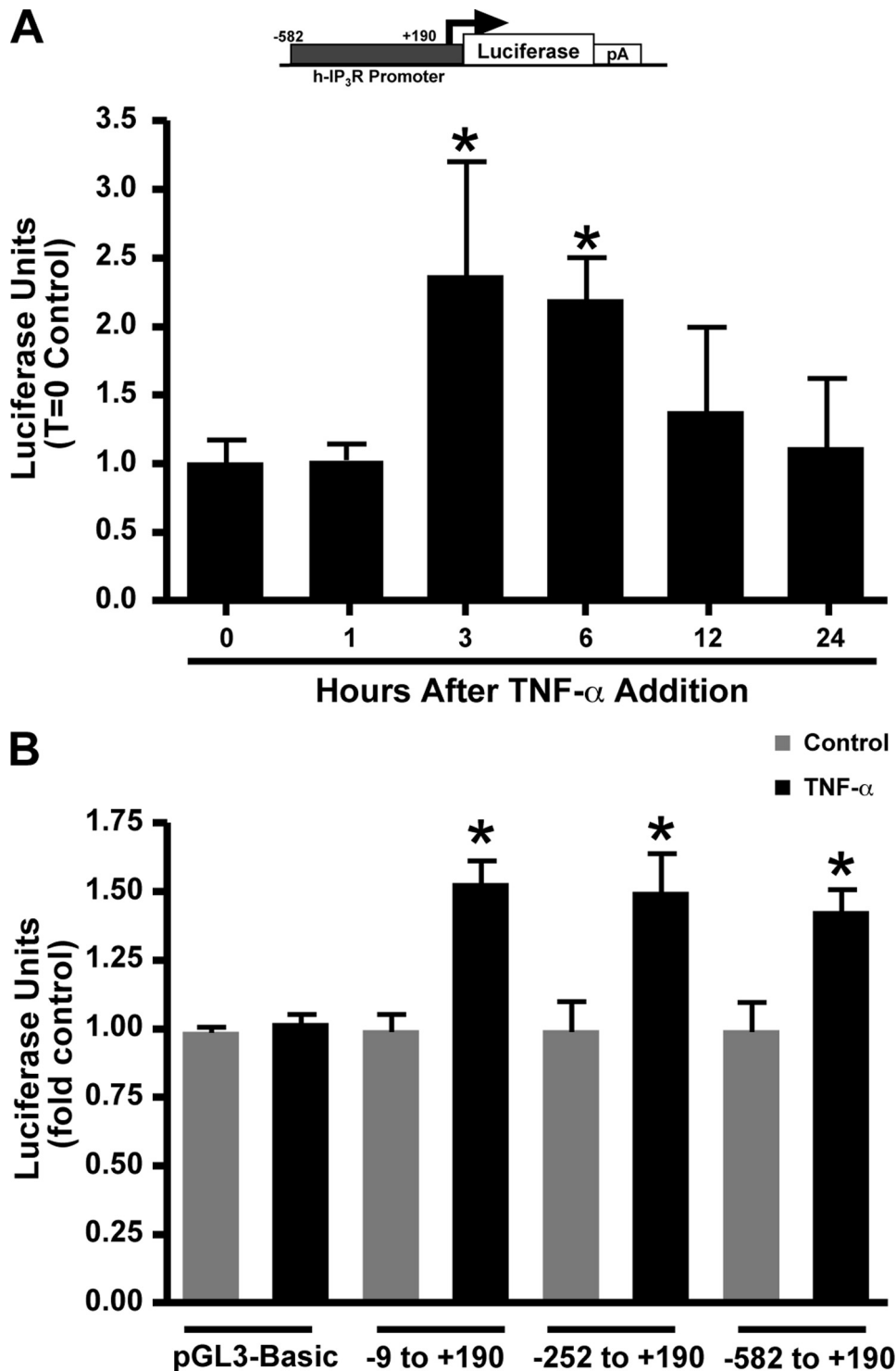
A

B

FIGURE 2. Enhanced IP₃R promoter activity with TNF-α addition. Constructs containing the −582 to +190 region of the human type-1 IP₃R promoter driving the expression of firefly luciferase were utilized to determine the ability of TNF-α to enhance IP₃R transcription. *A*, luciferase activity was tested at varying time points after 100 ng/ml TNF-α addition to obtain a temporal profile of regulation. *B*, deletion constructs were utilized to determine which region of the promoter was responsive to TNF-α regulation. Consistent luciferase activity observed 6 h after cytokine addition from each of the constructs suggested the −9 to +190 region as the site of regulation. Transfection efficiency was monitored by the co-transfection of a *Renilla* luciferase construct. $n = 6$ for each group. *Error bars* represent 1 S.D. and * indicates a *p* value < 0.01 obtained by a Bonferroni Multiple Comparison.

Regulation of the IP₃R Promoter Is Not Regulated by c-Jun—MatInspector software had suggested that the +59-bp site harbors a consensus AP-1 binding site. To determine if this site was regulated by c-Jun, a major component of AP-1, a dominant-negative (DN) c-Jun construct was employed (28). Again, the AP-1 reporter construct was utilized to confirm the ability of the c-Jun-DN to block AP-1 activity. Expression of ΔMEKK1 led to a significant increase in luciferase activity, which was inhibited in the presence of the c-Jun-DN gene (Fig. 5A). However, expression of c-Jun-DN and c-Jun imparted no effect on the enhanced luciferase activity observed with the full-length IP₃R promoter reporter in the presence of ΔMEKK1 expression and cytokine addition (Fig. 5, B and C). These data indicated that c-Jun was not playing a central role in the regulation IP₃R promoter activity by JNK.

Gel Shift Analyses Demonstrate SP-1 Binding at the +59-bp Site—Because the +59-bp site was implicated as being responsive to JNK activation, we sought to measure transcription factor binding to a probe derived from this region of the type-1 IP₃R promoter. Nuclear lysates obtained from Neuro2A cells significantly retarded the migration of a 42-bp probe containing the +59-bp site in electrophoretic mobility shift assays (EMSA, Fig. 6A). This binding was specific since it was competed away with the addition of a molar excess of non-radiolabeled probe. Additionally, when a radiolabeled probe mutated at the putative binding site (GAGAGGA-TGTGTTG) was utilized, no shifted complexes were observed (Fig. 6B). This suggested the nuclear extracts harbored a binding activity that specifically interacted with DNA sequences within this region. Moreover, addition of excess cold mutated probe did not compete away binding to the wild-type probe, indicating that factor binding

JNK regulation resides at the +59 bp site within the type-1 IP₃R promoter and that either AP-1 or SP-1 transcription factor binding could be key to this regulation.

was eliminated when the core site was ablated (Fig. 6B). Additionally, in agreement with the c-Jun-DN data described above, the addition of a cFos antibody failed to eliminate or shift the
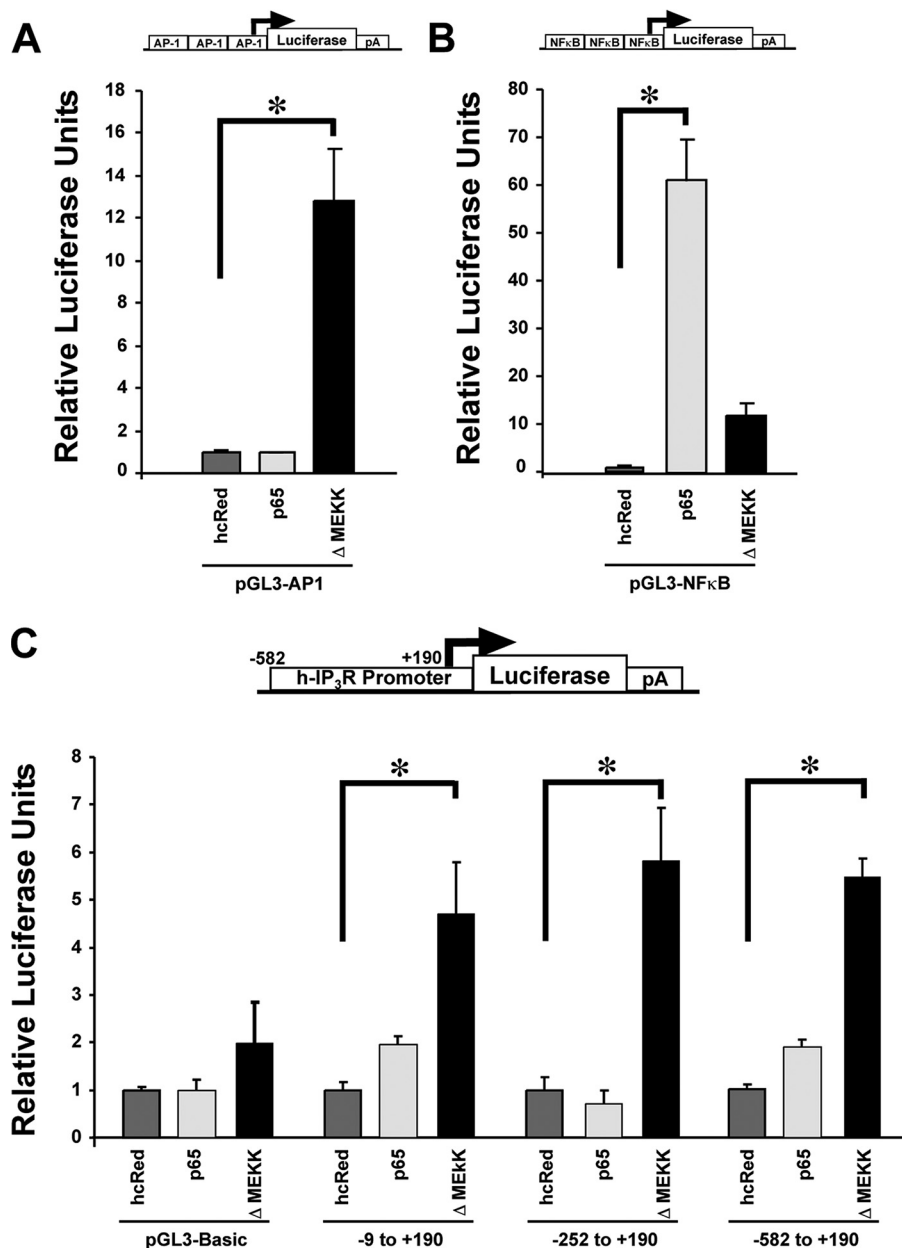
FIGURE 3. **Enhanced IP₃R promoter activity with JNK activation.** To identify which signaling pathway was primarily responsible for enhanced IP₃R promoter activity following TNF-α exposure, ΔMEKK1 and p65 expression plasmids were employed to separately activate JNK and NFκB signaling, respectively. *A*, plasmid harboring a concatenated AP-1 consensus binding sequence upstream of a luciferase reporter gene, pGL3-AP1, was utilized to confirm JNK-related activation by the ΔMEKK1 expression plasmid. *B*, second plasmid that contained a concatenated NFκB consensus binding sequence upstream of a luciferase reporter gene, pGL3-NFκB, was utilized to confirm NFκB-related activation by the p65 expression plasmid. *C*, luciferase reporter constructs that contained progressively shorter segments of the human IP₃R promoter upstream of the luciferase gene were co-transfected with either the ΔMEKK1 or NFκB expression plasmids and luciferase assays were performed 24-h later. Transient co-transfection of a control plasmid, hcRed, or the NFκB p65 expression construct with any of these IP₃R promoter deletion plasmids into Neuro2A cells did not significantly affect luciferase activity output, whereas co-transfection of the ΔMEKK1 construct resulted in significant enhancement of luciferase reporter gene expression from each of the three reporter plasmids. *Error bars* represent 1 S.E., and * indicates a *p* value < 0.01 by one-way ANOVA.

Dominant-negative SP-1 Blocks the TNF-α Enhancement of IP₃R-mediated Ca²⁺ Signals and Promoter Activity—To further examine the potential role SP-1 may play in the TNF-α enhancement in IP₃R mediated Ca²⁺ signals and promoter activity, we utilized a plasmid expressing a dominant-negative SP-1/glutathione *S*-transferase (GST) fusion protein (pSP1-DN) to block SP-1 activity (25, 29–31). The ability of dominant-negative SP-1 to block the enhancement of IP₃R promoter activity by TNF-α addition was determined by transfecting both the pSP1-DN and full-length IP₃R promoter luciferase constructs into Neuro2A cells (Fig. 7*A*). The dominant-negative SP-1 eliminated the enhanced promoter activity observed following cytokine addition. Next, the ability of the pSP1-DN construct to block the elevated IP₃R-mediated Ca²⁺ signals observed with TNF-α incubation was assessed. TNF-α exposure produced the characteristic enhancement of bradykinin-induced Ca²⁺ signals in Neuro2A cells transfected with the control pEBGN construct (Fig. 7, *B* and *C*). In contrast, TNF-α did not significantly affect IP₃R-mediated Ca²⁺ signals in cells expressing dominant-negative SP-1 (Fig. 7, *B* and *C*). These data, in aggregate, indicate that TNF-α enhances IP₃R-mediated Ca²⁺ signals and promoter activity through an SP-1-mediated process.

DISCUSSION

Our current work delineates a pathway by which TNF-α signaling can regulate the transcription of the type-1 IP₃R gene, thereby leading to greater Ca²⁺ release from the ER (18). Importantly, this increase in mRNA was sensitive to the JNK inhibitor SP600125, sug-

band corresponding to protein/DNA complex, further indicating AP-1 does not bind to the +59-bp site (Fig. 6*C*). Importantly, we observed a decrease in the intensity of the shifted band with SP-1 antibody incubation (Fig. 6*C*). This finding suggested SP-1 was a component of the shifted complex, and implicated SP-1 binding at the +59-bp site in TNF-α induced, JNK-mediated regulation of IP₃R expression.

gesting IP₃R mRNA levels are regulated through either an enhancement in transcription or a JNK-dependent regulation of type-1 IP₃R mRNA stability. Binding of the cytokine to its cell surface receptor leads to JNK activation, and phosphorylation of downstream transcription factors like AP-1 and SP-1 (32, 33). Our data indicate that the human type-1 IP₃R promoter contains a key SP-1 binding element 59 base
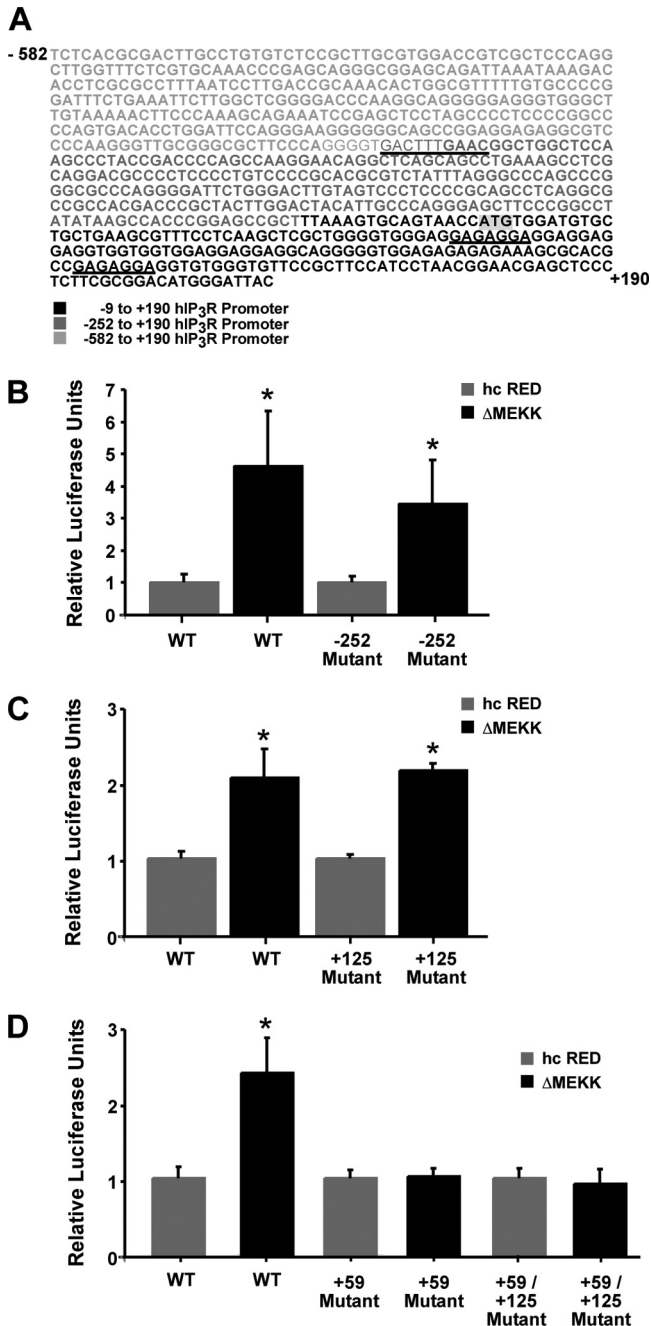
A

-582 TCTCACGCGACTTGCCTGTGTCTCCGCTTGCGTGGACCGTCGCTCCCAGG
CTTGGTTTCTCGTGCAAACCCGAGCAGGGCGGAGCAGATTAAATAAAGAC
ACCTCGCGCCTTTAATCCTTGACCGCAAACACTGGCGTTTTTGTGCCCCG
GATTTCTGAAATTCTTGGCTCGGGGACCCAAGGCAGGGGGAGGGTGGGCT
TGTAAAAACTTCCCAAAGCAGAAATCCGAGCTCCTAGCCCCTCCCCGGCC
CCAGTGACACCTGGATTCAGGGAAGGGGGGCAGCCGGAGGAGAGGCGTC
CCCAAGGGTTGCGGGCGCTTCCCAGGGGTGACTTTGAACGGCTGGCTCCA
AGCCCTACCGACCCCCAGCCAAGGAACAGGCTCAGCAGCCTGAAAGCCTCG
CAGGACGCCCCTCCCCTGTCCCCGCACGCGTCTATTTAGGGCCCAGCCCG
GGCGCCCAGGGGATTCTGGGACTTGTAGTCCCTCCCCGCAGCCCTCCACG
CCGCCACGACCCGCTACTTGGACTACATTGCCCAGGGAGCTTCCCGGCCT
ATATAAGCCACCCGGAGCCGCTTTAAAGTGCAGTAACCATGTGGATGTGC
TGCTGAAGCGTTTCCTCAAGCTCGCTGGGGTGGGAGGAGAGAGGAGGAGGAG
GAGGTGGTGGTGGAGGAGGAGGCAGGGGTTGGAGAGAGAGAAAGCCACG
CCGAGAGGAGGTGTGGGTGTTCCGCGTTCCATCCTAACGGAACGAGCTCCC
TCTTGCGGGACATGGGATTAC +190

■ -9 to +190 hIP₃R Promoter
■ -252 to +190 hIP₃R Promoter
■ -582 to +190 hIP₃R Promoter

FIGURE 4. **Site-specific activation of the IP₃R promoter by ΔMEKK1.** The regulation of the human type-1 IP₃R promoter with JNK activation was further analyzed using luciferase constructs containing wild type and mutated versions of the putative AP-1/SP-1 sites identified within the IP₃R promoter. *A*, 771-bp nucleotide sequence of the full-length human IP₃R promoter is shown, and the sequences corresponding to the location of the putative JNK-regulated sites are *underlined*. Luciferase reporter constructs that contain wild-type or mutated versions of the three predicted AP-1/SP-1 binding sites centered at -252 (*B*), $+59$ (*D*), and $+125$ bp (*C*) within human IP₃R promoter upstream of the luciferase gene were co-transfected with either the ΔMEKK1 expression plasmid or hcRed control plasmid, and luciferase assays were performed 24 h later. *Error bars* represent 1 S.E. $n = 6$ for each group, and * indicates a *p* value < 0.01 by one-way ANOVA.

FIGURE 5. **c-Jun-DN fails to block ΔMEKK1 enhancement of IP₃R promoter activity.** *A*, Neuro2A cells were co-transfected with c-Jun, a dominant-negative form of c-Jun (*cJun-DN*), and/or ΔMEKK1 expression plasmid along with a plasmid harboring concatenated AP-1 consensus binding sequence upstream of a luciferase reporter gene. Luciferase expression was assayed 24 h after transfection. *B*, Neuro2A cells were co-transfected with a c-Jun, c-Jun-DN, and/or ΔMEKK1 expression plasmid along with plasmid harboring the human IP₃R promoter sequence upstream of a luciferase reporter gene. An hcRed reporter gene-expressing plasmid was included as an internal control, and firefly luciferase activity was measured 24 h after transfection. *C*, Neuro2A cells were transfected with a c-Jun or c-Jun-DN along with the human IP₃R promoter reporter gene. Cultures were then incubated in the presence of 100 ng/ml TNF-α. Luciferase expression was assayed 6 h later. *Error bars* represent 1 S.E. * indicates a *p* value < 0.01 obtained by a Bonferroni Multiple Comparison test after significance was determined by one-way ANOVA.

pairs downstream of the putative transcription start site and mutation of this sequence abrogates SP-1 binding and JNK regulation. Additionally, the expression of a dominant-negative SP-1 was able to block the ability of TNF-α to affect 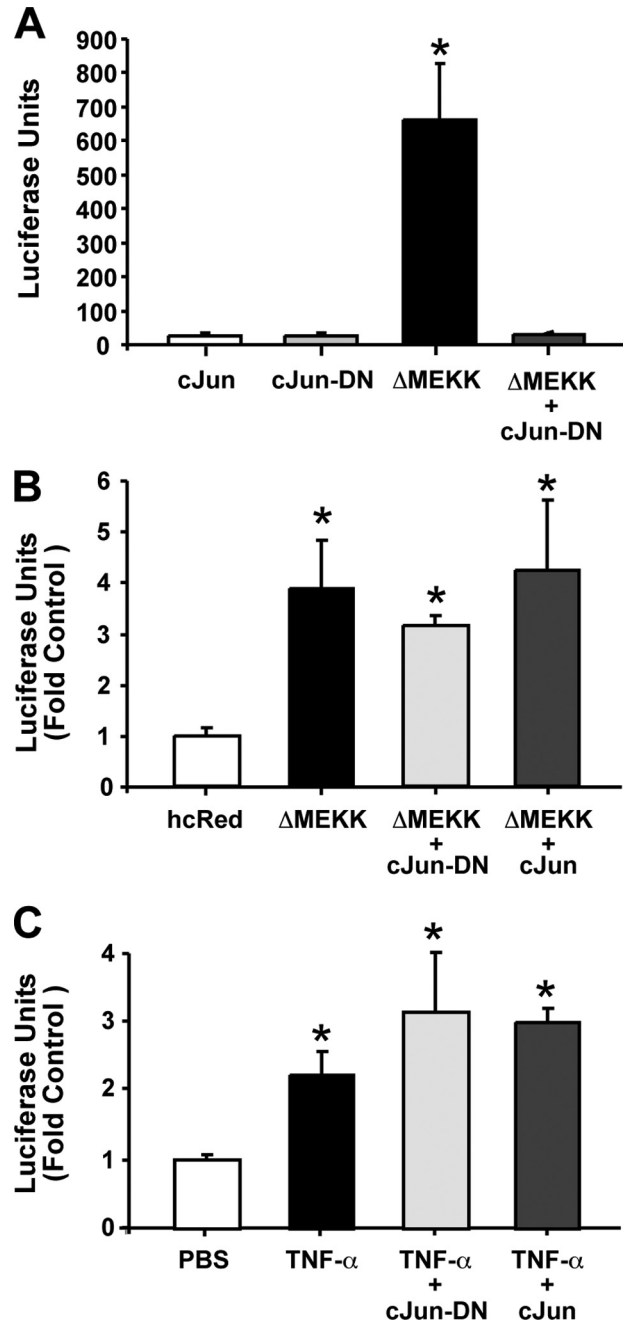IP₃R Ca²⁺ signals and promoter activity. These findings, in aggregate, uncover a novel pathway for the regulation of ER-derived Ca²⁺ signals during conditions of TNF-α-mediated neuroinflammation.

A

WT Probe: + + + + + + +
μg Lysate: 0 1 5 10 10 10 10
WT Cold: - - - - 5x 25x 100x

B

MT Probe: + + + + - - -
WT Probe: - - - - + + +
μg Lysate: 0 1 5 10 10 10 10
MT Cold: - - - - 5x 25x 100x

C

WT Probe: + + + + + +
μg Lysate: 10 10 10 10 10 10
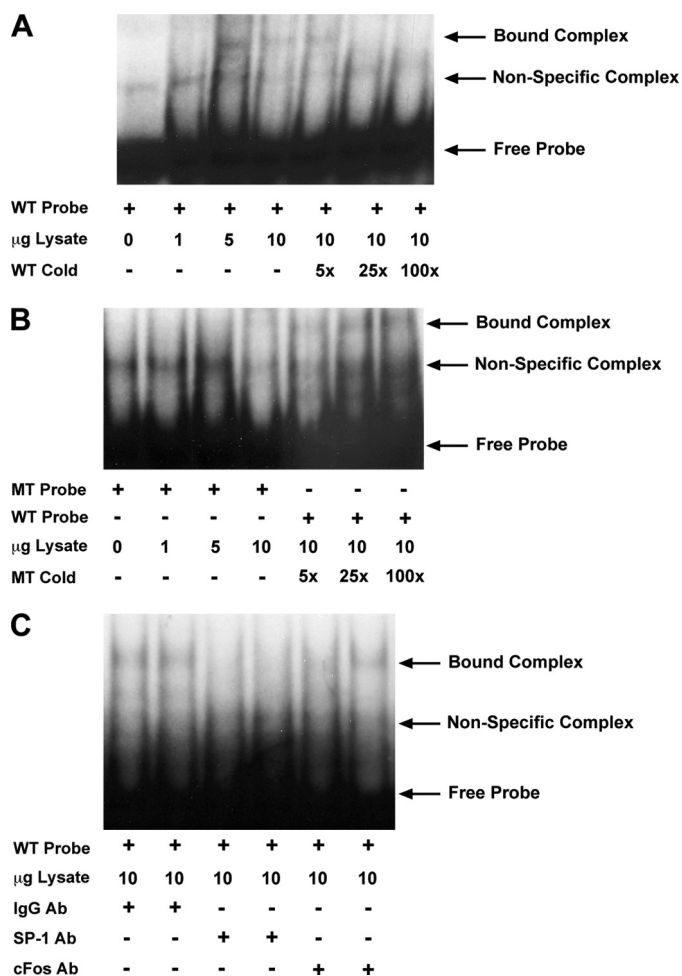IgG Ab: + + - - - -
SP-1 Ab: - - + + - -
cFos Ab: - - - - + +

FIGURE 6. **EMSA analyses indicate SP-1 binds to the +59-bp site within the human IP₃R promoter.** An EMSA was performed to ascertain transcription factor binding to a radioactively labeled 42-bp probe containing the putative +59-bp AP-1/SP-1 site identified within the human IP₃R promoter. *A,* increasing concentrations of untreated Neuro2A nuclear extracts (*lanes 2–4*), obtained by a salt gradient method, were utilized to examine transcription factor binding to 0.5 ng of ^{32}P-labeled probe. Protein binding is indicated by retardation in DNA probe migration and is designated in the figure by the bound complex arrow. Molar excess of wild-type control probe (*lanes 5–7*) was added to compete away the probe/protein interaction to illustrate the specificity of the shifted band. *B,* binding to a mutated probe was also assayed and the absence of a bound complex (*lanes 2–4*) indicated an elimination of transcription factor binding. To further test the binding affinity of the mutant probe, we assayed the ability of a molar excess of mutant cold probe to compete away the bound complex formed with the wild-type probe (*lanes 5–7*). *C,* during the binding reaction, 1 μg of a nonspecific IgG (*lanes 1* and *2*), c-Fos (*lanes 3* and *4*), or SP-1 antibody (*lanes 5* and *6*) was used to evaluate the respective antibodies ability to bind the transcription factor and compete with probe binding.

The cloning and sequencing of the mouse and human IP₃R promoter has been previously described (27, 34), and functional assays have indicated that the core promoter spans the putative transcription start site (−528 to +169 in mouse and −86 to +145 in the human homolog). These respective sequences are required to mimic the expression profile of endogenous IP₃R. Of particular interest is the high degree of homology between the murine and human type-1 IP₃R promoters in several regions including the +49 to +70 region, which contains the putative +59-bp SP-1 site characterized in the current study. Additionally, the sequence GAGAGGA, which was shown to be important for transcription factor binding to this region, is
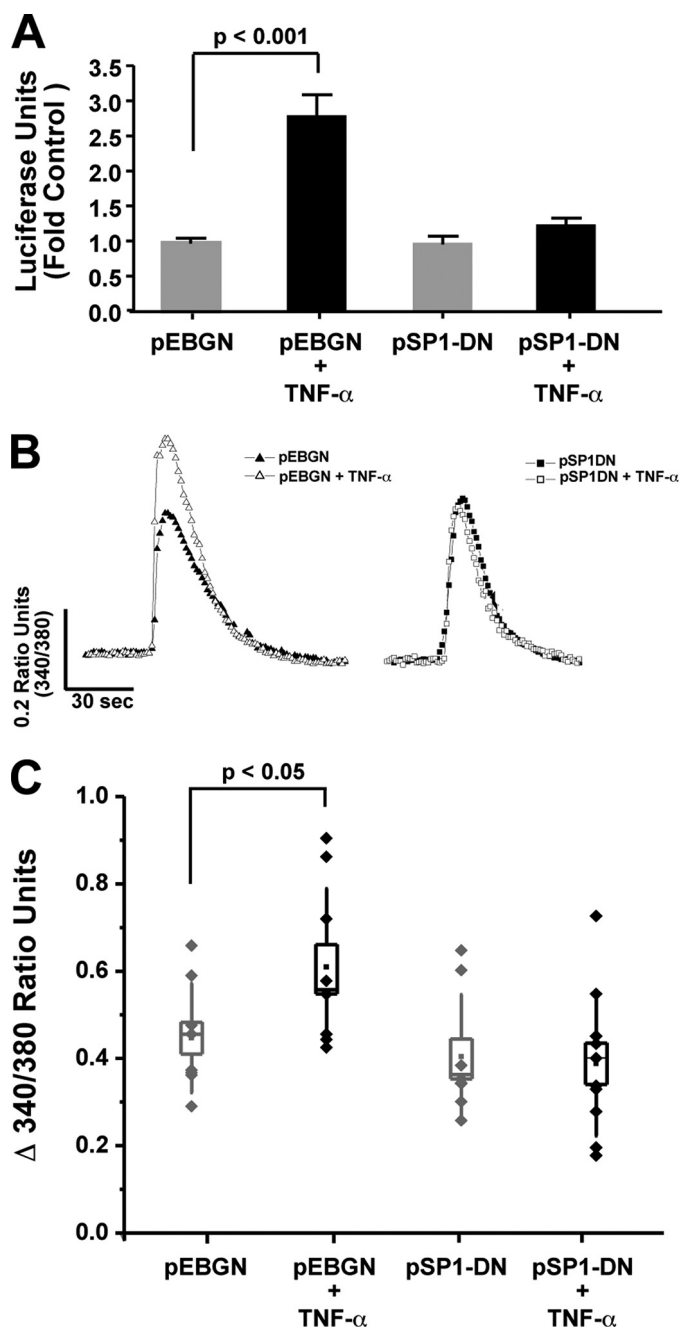

A

B

← pEBGN
△ pEBGN + TNF-α
■ pSP1DN
□ pSP1DN + TNF-α

C

FIGURE 7. **Dominant-negative SP-1 eliminates the ability of TNF-α to regulate the IP₃R promoter and enhance IP₃R-mediated Ca²⁺ signals.** Neuro2A cells were transiently transfected with pSP1-DN, a plasmid expressing a dominant-negative SP-1 fused to GST, or a control GST-nuclear localization signal construct (*pEBGN*). *A,* Neuro2A cells were co-transfected with pSP1-DN or pEBGN and the full-length IP₃R promoter luciferase construct, and subsequently incubated with TNF-α for 6 h. Relative luciferase activity is shown. *B* and *C,* Neuro2A cells transfected as described above were subjected to Ca²⁺ imaging with Fura2, 24 h after TNF-α incubation. Sample traces from individual neurons and collective data obtained from coverslip averages is illustrated. *p* values were obtained by a Bonferroni Multiple Comparison test after significance was determined by one-way ANOVA. Box plot parameters: *dots* represent coverslip averages, the *center* of the box is the mean of the data, the *edge* of the box is 1 S.E., *whiskers* are 1 S.D.

found in the mouse, human, rat, and bovine promoters but not the *Xenopus* and *Drosophila* IP₃R genes, with the latter having a similar but altered GAGACGGA site. It should be noted that although both of these sequences deviate from the consensus GGGGCG-

GGGC SP-1 binding sequence, this transcription factor has been shown to bind to a slightly altered sequence, AAGAGGCGGG, which shares significant similarity to the +59-bp IP$_3$R site (35, 36). In addition, this region is proximally located downstream of a highly GC-rich sequence, suggesting this binding site may represent one of several SP-1 binding sites in the promoter.

The transcription factor SP-1 is regulated by its phosphorylation state (37), and several groups have shown that it is regulated by MAPK-dependent pathways, including those downstream of TNF-R activation (33, 38). Notably, inhibitors of JNK activity can block SP-1 activation, and thereby alter SP-1-dependent gene expression (33). Our gel shift assays demonstrated that this transcription factor is a component of a binding activity derived from Neuro2A nuclear extracts, while expression of dominant-negative SP-1 eliminated the ability of TNF-α to enhance IP$_3$R-mediated Ca^{2+} signals and promoter activity. This evidence indicates SP-1 represents the binding factor responsible for JNK regulation of the IP$_3$R promoter. Future research utilizing mutants that lack critical serine/threonine residues believed to underlie SP-1 activation in neuronal cells will undoubtedly further help to elucidate its role in this signaling pathway.

It is also important to note that other putative transcription factor binding sites also lie within the highly conserved regions of the IP$_3$R promoter, including an AP-2 site that is believed to be a site of retinoic acid regulation and an E-box motif for basic helix-loop-helix (bHLH) transcription factors (27, 39). Differential transcription factor binding to these highly conserved sites facilitates specific expression patterns of the type-1 IP$_3$R within the CNS, including high levels of expression in the cerebellum and the CA1 region of the hippocampus (40). Notably, the latter brain region has been shown to be deleteriously affected by Alzheimer disease (AD), and our group has demonstrated that TNF-α is produced from microglia and neurons residing within this region in a mouse model of AD (41). It will be of interest to determine if IP$_3$R expression is altered by TNF-α during AD pathogenesis because several groups have implicated altered IP$_3$R signaling in AD (42–44).

Very few studies have examined how the physiological regulation of IP$_3$R expression may affect IP$_3$-derived Ca^{2+} signals. Several reports have described how factors like all-*trans*-retinoic acid and phospholipid scramblase 1 may alter expression through regulation of IP$_3$R transcription (22, 45). However, these studies have yet to examine the effect of this increase in receptor expression on inositol-mediated Ca^{2+} signals. To address this question, others have examined IP$_3$R stably transfected cell lines and have shown that an 8-fold increase of the IP$_3$R protein in L fibroblasts leads to a modest, but significant, increase in total Ca^{2+} release (46). However, these experiments did not fully elucidate the importance of receptor number on Ca^{2+} release, since stable overexpression of the receptor may mask the requisite co-factors or scaffolding proteins necessary for proper location and maximal Ca^{2+} release. Another way one could examine the effect of IP$_3$R expression on ER Ca^{2+} release is by comparing the differences in release kinetics in two different cell types that express differing levels of the channel. Our group has observed that when comparing two similar exocrine cells, parotid acini exhibit a shorter latency, faster rise time to peak, and higher maximal Ca^{2+} release than pancreas

acini possibly due to a 4-fold higher expression of IP$_3$R (47). Our current work examines the effect of increasing IP$_3$R expression through an endogenous SP-1-mediated transcription event on ER Ca^{2+} release within a single cell type. To the best of our knowledge this is the first such study, and represents an important step in understanding how a physiological alteration in IP$_3$R expression may influence ER-derived Ca^{2+} signals.

The enhancement of Ca^{2+} signals downstream of Gα$_q$ activation may not only be due to an enhancement of IP$_3$R mRNA and protein, but also as a result of the simultaneous enhancement in proteins that direct localization and stabilize the receptor to facilitate maximal release. The expression of these factors, in addition to the enhanced expression of the channel itself, may have altered other kinetics parameters such as the potency to IP$_3$, the latency, and time to peak of the Ca^{2+} release event. These alterations could result in significant physiological consequences, where an enhancement of IP$_3$ potency may selectively mediate Ca^{2+} release in cells exposed to TNF-α, but fail to initiate a release event in cells that have not been exposed to the cytokine. Further research focused on identification of additional SP-1- or AP-1-responsive genes regulated by TNF-α will further elucidate the physiological implication of this pathway and will likely shed light on other inflammatory mediators that may act comparably.

Inflammation within the CNS has been shown previously to regulate several other pathways important in neuronal signaling. Exposure to pro-inflammatory cytokines, TNF-α and IL-1β, inhibits the induction of long-term potentiation, an electrophysiologic correlate to learning and memory, within the CA1 region of the hippocampus (10). Cytokine-based inhibition in these instances can occur through another Ca^{2+} channel, the *N*-methyl-D-aspartic acid receptor. This pathway was found to require p38, a mitogen-activated protein kinase, which is activated in a similar manner to JNK observed in our study (11). Additionally, TNF-α also regulates the insertion of Ca^{2+} permeable AMPA receptors in hippocampal neurons, again demonstrating that inflammation can dramatically alter the Ca^{2+} signaling environment of neurons (48). However, cytokine signaling may not always be detrimental since mice genetically altered to not express functional TNF receptors demonstrate an impairment in LTP (49). This at least suggests that the physiological production of TNF-α is necessary to ensure healthy synapses. In either case, cytokines have been shown to significantly influence neuronal communication, and strict control over their expression levels/patterns is undoubtedly important in determining how physiologic outcomes impart a positive or negative influence on neuronal function. Future research efforts will further examine the role inflammatory cytokines in shaping neuronal signals observed during periods of chronic neuroinflammation.

REFERENCES

1. Di Filippo, M., Sarchielli, P., Picconi, B., and Calabresi, P. (2008) *Trends Pharmacol. Sci.* **29,** 402–412
2. Allan, S. M., and Rothwell, N. J. (2001) *Nat. Rev. Neurosci.* **2,** 734–744
3. Carswell, E. A., Old, L. J., Kassel, R. L., Green, S., Fiore, N., and Williamson, B. (1975) *Proc. Natl. Acad. Sci. U.S.A.* **72,** 3666–3670
4. Kriegler, M., Perez, C., DeFay, K., Albert, I., and Lu, S. D. (1988) *Cell* **53,** 45–53
5. Black, R. A., Rauch, C. T., Kozlosky, C. J., Peschon, J. J., Slack, J. L., Wolfson, M. F., Castner, B. J., Stocking, K. L., Reddy, P., Srinivasan, S., Nelson, N., Boiani, N., Schooley, K. A., Gerhart, M., Davis, R., Fitzner, J. N., Johnson, R. S., Paxton, R. J., March, C. J., and Cerretti, D. P. (1997) *Nature* **385,** 729–733
6. Hanisch, U. K. (2002) *Glia.* **40,** 140–155
7. Kinouchi, K., Brown, G., Pasternak, G., and Donner, D. B. (1991) *Biochem. Biophys. Res. Commun.* **181,** 1532–1538
8. Chen, G., and Goeddel, D. V. (2002) *Science* **296,** 1634–1635
9. Schneider-Brachert, W., Tchikov, V., Neumeyer, J., Jakob, M., Winoto-Morbach, S., Held-Feindt, J., Heinrich, M., Merkel, O., Ehrenschwender, M., Adam, D., Mentlein, R., Kabelitz, D., and Schütze, S. (2004) *Immunity.* **21,** 415–428
10. Cunningham, A. J., Murray, C. A., O'Neill, L. A., Lynch, M. A., and O'Connor, J. J. (1996) *Neurosci. Lett.* **203,** 17–20
11. Butler, M. P., O'Connor, J. J., and Moynagh, P. N. (2004) *Neuroscience* **124,** 319–326
12. Bootman, M. D., Collins, T. J., Peppiatt, C. M., Prothero, L. S., MacKenzie, L., De Smet, P., Travers, M., Tovey, S. C., Seo, J. T., Berridge, M. J., Ciccolini, F., and Lipp, P. (2001) *Semin. Cell Dev. Biol.* **12,** 3–10
13. Betzenhauser, M. J., Wagner, L. E., 2nd, Iwai, M., Michikawa, T., Mikoshiba, K., and Yule, D. I. (2008) *J. Biol. Chem.* **283,** 21579–21587
14. Iino, M. (1991) *J. Gen. Physiol.* **98,** 681–698
15. Ferris, C. D., Cameron, A. M., Bredt, D. S., Huganir, R. L., and Snyder, S. H. (1991) *Biochem. Biophys. Res. Commun.* **175,** 192–198
16. Giovannucci, D. R., Groblewski, G. E., Sneyd, J., and Yule, D. I. (2000) *J. Biol. Chem.* **275,** 33704–33711
17. Sneyd, J., Tsaneva-Atanasova, K., Bruce, J. I., Straub, S. V., Giovannucci, D. R., and Yule, D. I. (2003) *Biophys. J.* **85,** 1392–1405
18. Park, K. M., Yule, D. I., and Bowers, W. J. (2008) *J. Biol. Chem.* **283,** 33069–33079
19. Stutzmann, G. E., LaFerla, F. M., and Parker, I. (2003) *J. Neurosci.* **23,** 758–765
20. Takei, N., and Endo, Y. (1994) *Brain Res.* **652,** 65–70
21. Dieckmann-Schuppert, A., and Schnittler, H. J. (1997) *Cell Tissue Res.* **288,** 119–126
22. Zhou, Q., Ben-Efraim, I., Bigcas, J. L., Junqueira, D., Wiedmer, T., and Sims, P. J. (2005) *J. Biol. Chem.* **280,** 35062–35068
23. Ramirez, S. H., Sanchez, J. F., Dimitri, C. A., Gelbard, H. A., Dewhurst, S., and Maggirwar, S. B. (2001) *J. Neurochem.* **78,** 874–889
24. Leppä, S., Eriksson, M., Saffrich, R., Ansorge, W., and Bohmann, D. (2001) *Mol. Cell Biol.* **21,** 4369–4378
25. Al-Sarraj, A., Day, R. M., and Thiel, G. (2005) *J. Cell Biochem.* **94,** 153–167
26. Fanger, G. R., Johnson, N. L., and Johnson, G. L. (1997) *EMBO J.* **16,** 4961–4972
27. Deelman, L. E., Jonk, L. J., and Henning, R. H. (1998) *Gene* **207,** 219–225
28. Brown, P. H., Chen, T. K., and Birrer, M. J. (1994) *Oncogene* **9,** 791–799
29. Puebla, C., Farías, M., González, M., Vecchiola, A., Aguayo, C., Krause, B., Pastor-Anglada, M., Casanello, P., and Sobrevia, L. (2008) *J. Cell Physiol.* **215,** 645–656
30. Wu, D. Y., and Yao, Z. (2006) *Cell Res.* **16,** 319–322
31. Kavurma, M. M., and Khachigian, L. M. (2003) *J. Biol. Chem.* **278,** 32537–32543
32. Pulverer, B. J., Kyriakis, J. M., Avruch, J., Nikolakaki, E., and Woodgett, J. R. (1991) *Nature* **353,** 670–674
33. Benasciutti, E., Pagès, G., Kenzior, O., Folk, W., Blasi, F., and Crippa, M. P. (2004) *Blood* **104,** 256–262
34. Furutama, D., Shimoda, K., Yoshikawa, S., Miyawaki, A., Furuichi, T., and Mikoshiba, K. (1996) *J. Neurochem.* **66,** 1793–1801
35. Letovsky, J., and Dynan, W. S. (1989) *Nucleic Acids Res.* **17,** 2639–2653
36. Jolliff, K., Li, Y., and Johnson, L. F. (1991) *Nucleic Acids Res.* **19,** 2267–2274
37. Chu, S., and Ferro, T. J. (2005) *Gene.* **348,** 1–11
38. Koga, T., Kuwahara, I., Lillehoj, E. P., Lu, W., Miyata, T., Isohama, Y., and Kim, K. C. (2007) *Am. J. Physiol. Lung Cell Mol. Physiol.* **293,** L693–L701
39. Konishi, Y., Kobayashi, Y., Kishimoto, T., Makino, Y., Miyawaki, A., Furuichi, T., Okano, H., Mikoshiba, K., and Tamura, T. (1997) *J. Neurochem.* **69,** 476–484
40. Furuichi, T., Simon-Chazottes, D., Fujino, I., Yamada, N., Hasegawa, M., Miyawaki, A., Yoshikawa, S., Guénet, J. L., and Mikoshiba, K. (1993) *Receptors Channels* **1,** 11–24
41. Janelsins, M. C., Mastrangelo, M. A., Oddo, S., LaFerla, F. M., Federoff, H. J., and Bowers, W. J. (2005) *J. Neuroinflammation* **2,** 23
42. Cheung, K. H., Shineman, D., Müller, M., Cárdenas, C., Mei, L., Yang, J., Tomita, T., Iwatsubo, T., Lee, V. M., and Foskett, J. K. (2008) *Neuron.* **58,** 871–883
43. Stutzmann, G. E., Caccamo, A., LaFerla, F. M., and Parker, I. (2004) *J. Neurosci.* **24,** 508–513
44. Leissring, M. A., Parker, I., and LaFerla, F. M. (1999) *J. Biol. Chem.* **274,** 32535–32538
45. Bradford, P. G., and Autieri, M. (1991) *Biochem. J.* **280,** 205–210
46. Mackrill, J. J., Wilcox, R. A., Miyawaki, A., Mikoshiba, K., Nahorski, S. R., and Challiss, R. A. (1996) *Biochem. J.* **318,** 871–878
47. Giovannucci, D. R., Bruce, J. I., Straub, S. V., Arreola, J., Sneyd, J., Shuttleworth, T. J., and Yule, D. I. (2002) *J. Physiol.* **540,** 469–484
48. Ogoshi, F., Yin, H. Z., Kuppumbatti, Y., Song, B., Amindari, S., and Weiss, J. H. (2005) *Exp. Neurol.* **193,** 384–393
49. Albensi, B. C., and Mattson, M. P. (2000) *Synapse* **35,** 151–159